Research Article | Vol. 26, No. 26 | 24 Dec 2018 | OPTICS EXPRESS 34569
Optics EXPRESS

Fast Fresnel propagation through a set of inclined reflecting planes applicable for X-ray imaging

STANISLAV HRIVŇAK,[1,*] JOZEF ULIČNÝ,[1] AND PATRIK VAGOVIČ[2,3]

[1]Department of Biophysics, Faculty of Science, P. J. Šafárik University, Jesenná 5, 04154 Košice, Slovakia
[2]European XFEL GmbH, Holzkoppel 4, 22869 Schenefeld, Germany
[3]Center for Free-Electron Laser Science, DESY, Notkestrasse 85, 22607 Hamburg, Germany
[*]stanislav.hrivnak@student.upjs.sk

Abstract: We present a fast and accurate method for wave propagation through a set of inclined reflecting planes. It is based on the coordinate transformation in reciprocal space leading to a diffraction integral, which can be calculated only by using two 2D Fast Fourier Transforms and one 2D interpolation. The method is numerically tested, and comparisons with standard methods show its superiority in both computational speed and accuracy. The direct application of this method is found in the X-ray phase contrast imaging using the Bragg magnifier—an optics consisting of crystals asymmetrically diffracting in Bragg geometry.

1. Introduction

Many applications of electromagnetic radiation rely on the accurate description of the wave propagation through the air or an arbitrary medium. One of these applications is the X-ray phase contrast imaging, where the wave propagation plays an exceptionally important role. The reason for this mainly comes from the phase problem, where one often needs to perform many forward and backward wave propagations in order to solve the nontrivial inverse problem [1]. Because of the huge increase in data production rates due to advanced modern X-ray sources (synchrotrons and free electron lasers), the need for fast and accurate wave propagations (as a part of data interpretation) is currently an important bottleneck. The speed of the process can be enhanced by hardware or software improvements. This study focuses on software by introducing a computationally efficient and very accurate approach for a specific case of wave propagation through a set of inclined reflecting planes.

For wave propagation in isotropic and homogenous media, one can conveniently use the scalar diffraction theory working with only one complex scalar function of space and time, which fully describes the electromagnetic disturbance [2]. This function, which is often simply termed as wave-field, contains information about the wave's amplitude and phase for a given point in spacetime. The simplest and the most common case of wave propagation is between two parallel planes. This can be easily performed using a convolution operator, which is in practice accomplished by adapting the Fast Fourier Transform (FFT) - a well-known algorithm for its great efficiency and time complexity.

The situation is different for wave propagation on an inclined plane, where the distance between the planes is not constant. Therefore, one cannot use FFT and benefit from its favorable computational scaling. Various solutions to this problem have been suggested. In Chapter 2, we present two standard approaches for comparison: one optimizing for speed but with limited accuracy (used in [3, 4]), and one exact treatment using heavy computational demands (used e.g. in [5]).

Another approach based on Rayleigh–Sommerfeld integral was proposed in [6, 7]. It uses similar theoretical treatment as presented in this paper with comparable results, and can be viewed as an alternative method for the wave propagation on an inclined plane. From the computational

#336396 https://doi.org/10.1364/OE.26.034569
Journal © 2018 Received 28 Jun 2018; revised 16 Nov 2018; accepted 20 Nov 2018; published 20 Dec 2018

Optics EXPRESS

point of view, both alternative approaches use two 2D FFT's and one 2D interpolation in reciprocal space. However, our approach further generalizes the formalism in two ways. First, it provides relationships allowing wave-field propagation *through* an inclined reflecting plane (see Fig. 1) with the same computational demands as for a propagation *on* an inclined plane. Second, it generalizes the mathematical treatment for propagation through any number of consecutive inclined reflecting planes (crystals) while still using just two 2D FFT's and one 2D interpolation.

This paper also closely relates to [8], where the developed formalism is the same as presented here, but only for a 1D case. Even though the authors of that paper further generalized the treatment also for a 2D case in a short notice, it is done in an incorrect manner. Chapter 2.3 provides a correct derivation and further extends the formalism as stated in the previous paragraph.

The application of our method is readily found in the fast and accurate forward and backward propagation through the Bragg magnifier [9], which consists of 2 or 4 crystals (reflecting planes) yielding magnified image in both directions by means of asymmetrical Bragg diffraction. Our developed method is intended to be used for phase retrieval of the X-ray images obtained by Bragg magnifier in microtomographic measurements [3, 10]. Since our primary motivation is focused on the X-ray wave propagation, the inclined reflecting planes will be from now on referred to as crystals, although they are not the only possible application.

The paper is organized as follows. Chapter 2 fully describes wave propagation through one crystal for three methods – Effective distance method, Many Fourier Transforms method and the novel method called Reciprocal coordinate transformation method. We also cover the inclusion of the crystal transfer functions in the calculation. Chapter 3 presents the generalization of the formalism for an arbitrary number of crystals, and Chapter 4 shows the results of the numerical tests of the developed method in comparison with other two described methods. Finally, the paper finishes with Conclusions.

2. Propagation through one crystal

Let us first treat the case of one reflecting plane (crystal) magnifying the beam in vertical (x) direction (Fig. 1). We define three Cartesian coordinate systems over three planes of interest - object plane (right after the sample, perpendicular to the main beam direction) coordinates (x_0, y_0), crystal plane coordinates (x_1, y_1) and the detector plane coordinates (x_2, y_2). The dual (reciprocal) coordinates to them will be denoted as $(\tilde{x}_0, \tilde{y}_0)$, $(\tilde{x}_1, \tilde{y}_1)$ and $(\tilde{x}_2, \tilde{y}_2)$, respectively, and the corresponding complex scalar wave-fields over these planes as $U_0(x_0, y_0)$, $U_C(x_1, y_1)$ and $U_D(x_2, y_2)$. Let us denote the mean propagation distance between the object and the crystal plane as z_0, and between the crystal plane and the detector plane as z_1. Let the angles of the incoming and outcoming beam with respect to the inclined plane be α and β as drawn in Fig. 1.

The definition of the direct 2D Fourier transform of a function $f(x, y)$ for our purposes will be

$$\widetilde{f}(\tilde{x}, \tilde{y}) = \frac{1}{(2\pi)^2} \int_{-\infty}^{\infty} f(x, y) \exp\left[-i\left(\tilde{x}x + \tilde{y}y\right)\right] dxdy \tag{1}$$

with the corresponding inverse Fourier transform

$$f(x, y) = \mathcal{F}^{-1}\left[\widetilde{f}(\tilde{x}, \tilde{y})\right] = \int_{-\infty}^{\infty} \widetilde{f}(\tilde{x}, \tilde{y}) \exp\left[i\left(\tilde{x}x + \tilde{y}y\right)\right] d\tilde{x}d\tilde{y}. \tag{2}$$

Our goal is to find a method for fast and precise propagation between the object plane (described by $U_0(x_0, y_0)$) and the detector plane (described by $U_D(x_2, y_2)$). Methodologically, it is important to distinguish between different imaging regimes based on the Fresnel number $N_F = b^2/(\lambda z)$, where b is the linear size of the sample, λ is the radiation wavelength and z is the effective propagation distance. We will restrict our considerations to the Fresnel regime (paraxial

Optics EXPRESS

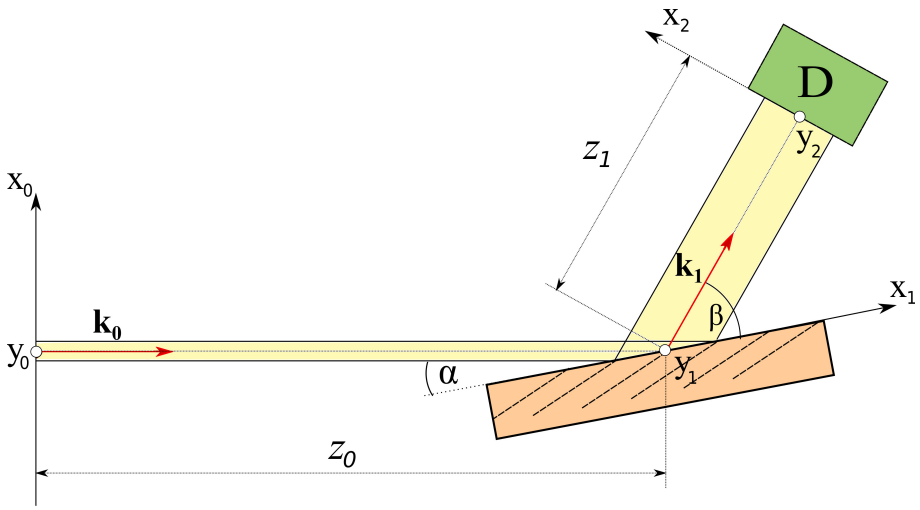

Fig. 1. Wave propagation through the reflecting inclined plane - crystal (in orange) from sample plane (left) to the detector D. The sketch represents the one-crystal geometry situation from the side view. The axis y_0, y_1 and y_2 are perpendicular to the figure plane. The dashed lines correspond to the active diffraction planes of the crystal.

approximation) for which $N_F \gg 1$, because most of the applications we aim for safely satisfy this condition. If that is not the case, our proposed method can also be easily generalized for the case of the exact free space propagator. We will further assume that, in general, asymmetric Bragg reflection occurs, i.e. $\alpha \neq \beta$, since the reflection is effectively happening with respect to the crystal lattice planes (dashed lines in Fig. 1). The magnification factor of the beam is defined as $M = \sin\beta/\sin\alpha$. More details about the phenomenon of Bragg reflection in perfect crystals can be found in [11, 12].

In the following paragraphs, we will present three possible methods to accomplish our goal of propagation through reflecting inclined planes. The first method, which we call *Many Fourier transforms*, will serve as a reference since it is based on well-established and accurate methods for free space propagation between parallel planes. The second method, which we call *Effective distances*, is the one commonly used to approximate our considered propagation problem and the third method is our new proposed method itself.

2.1. Many Fourier Transforms method (MFT)

Imagine all three defined wave-fields U_0, U_C and U_D are sampled on a uniform grid of size $L \times L$. Their discretized versions will be denoted using indices $i, j \in \{1, 2, \ldots, L\}$, e.g. $U_0(x_0^{(i)}, y_0^{(j)})$.

If we are interested in the i-th row of the crystal plane wave-field $U_C(x_1^{(i)}, y_1)$, we need to perform standard Fresnel propagation between parallel planes with a mutual distance $z_0^{(i)} = z_0 + x_1^{(i)} \cos\alpha$. The i-th row of the result will give us the desired values for $U_C(x_1^{(i)}, y_1)$ (while discarding all the other rows). This needs to be repeated for all L rows yielding $U_C(x_1, y_1)$ for all the grid points. Mathematically, for $\forall i$

$$U_C(x_1^{(i)}, y_1) = \left(\mathcal{F}^{-1} \left\{ \widetilde{U}_0(\tilde{x}_0, \tilde{y}_0) \exp\left[-\frac{i z_0^{(i)}}{2K} \left(\tilde{x}_0^2 + \tilde{y}_0^2 \right) \right] \right\} \right)^{(i)}, \tag{3}$$

where the exponential term is the Fresnel propagator, exponent (i) denotes extracting the i-th row of the wave-field and $K = 2\pi/\lambda$ is the wavevector.

Optics EXPRESS

Further propagation from the crystal plane to the detector plane will be performed in the following manner. Let us define a 2D wave-field

$$ {}^{i}U_C^{(0)}(x_2, y_2) = \begin{cases} U_C(x_1^{(i)}, y_1) \dots & i\text{−th row,} \\ 0 \dots\dots & \text{elsewhere.} \end{cases} \tag{4} $$

Based on the Huygens principle, we can decompose the wave-field U_C as

$$ U_C(x_1, y_1) = \sum_{i=1}^{L} {}^{i}U_C^{(0)}(x_2, y_2) \tag{5} $$

and propagate each term in the sum again by means of the standard Fresnel propagation between parallel planes as

$$ U_D(x_2, y_2) = \sum_{i=1}^{L} \mathcal{F}^{-1} \left\{ {}^{i}\widetilde{U}_C^{(0)}(x_2, y_2) \exp\left[-\frac{i z_1^{(i)}}{2K} \left(\tilde{x}_2^2 + \tilde{y}_2^2 \right) \right] \right\}, \tag{6} $$

where $z_1^{(i)} = z_1 + x_1^{(i)} \cos\beta$ is the propagation distance for the i-th plane in the above decomposition.

This method is straightforward and precise but requires at least $3L + 1$ evaluations of 2D Fourier transform. Therefore, it is not suitable for the problems where one needs to propagate the wave-fields many times, e.g. in phase retrieval problems. Still, we will use this method as a reference when testing other methods.

2.2. Effective distances method (ED)

This simplified method neglects the effect of varying propagation distances and only uses the standard Fresnel propagation between parallel planes with the mean (effective) propagation distances z_0 and z_1. The relationship between U_D and U_0 can, therefore, be written as

$$ U_D(x_2, y_2) = \mathcal{F}^{-1} \left\{ \widetilde{U}_0(\tilde{x}_0, \tilde{y}_0) \exp\left[-\frac{i z_0}{2K} \left(\tilde{x}_0^2 + \tilde{y}_0^2 \right) \right] \exp\left[-\frac{i z_1}{2K} \left(\tilde{x}_2^2 + \tilde{y}_2^2 \right) \right] \right\}. \tag{7} $$

Using the relationship $\tilde{x}_2 = \tilde{x}_0 / M$ for compressing the frequencies after magnification, we can simplify the equation to

$$ U_D(x_2, y_2) = \mathcal{F}^{-1} \left\{ \widetilde{U}_0(\tilde{x}_0, \tilde{y}_0) \exp\left[-\frac{i \left[\left(z_0 + \frac{z_1}{M^2} \right) \tilde{x}_0^2 + (z_0 + z_1) \tilde{y}_0^2 \right]}{2K} \right] \right\}. \tag{8} $$

This method requires just two 2D FFT's, which drastically reduces the computational demands. On the other hand, the approximation of average propagation distance can cause severe artifacts, e.g., in the cases of short propagation distances or large beams, when the propagation distances within the upper and lower parts of the beam differ significantly.

2.3. Reciprocal coordinates transformation method (RCT)

Now we proceed to our proposed method. Let us write down the scalar diffraction formula in Fresnel approximation for the case of propagation from the object plane to the crystal plane in (x_0, y_0) coordinates

$$ U_C(x_0, y_0) = \iint \widetilde{U}_0(\tilde{x}_0, \tilde{y}_0) \exp\left[-i \frac{z_0 + z(x_0)}{2K} \left(\tilde{x}_0^2 + \tilde{y}_0^2 \right) \right] \exp\left[i(\tilde{x}_0 x_0 + \tilde{y}_0 y_0) \right] d\tilde{x}_0 d\tilde{y}_0, \tag{9} $$

Optics EXPRESS

where $z(x_0)$ is the deviation from the mean propagation distance z_0. This integral cannot be evaluated by a simple Fourier transform (because of the dependence of the integral kernel on x_0). From Fig. 1 we get $x_0 = x_1 \sin\alpha$, $y_1 = y_0$ and $z(x_0) = x_1 \cos\alpha$ and after substituting it in Eq. (9) and rearranging we arrive at

$$U_C(x_1, y_1) = \iint \widetilde{U}_0(\tilde{x}_0, \tilde{y}_0) \exp\left[-i\frac{z_0}{2K}\left(\tilde{x}_0^2 + \tilde{y}_0^2\right)\right] \times \exp\left\{ i x_1 \underbrace{\left[\tilde{x}_0 \sin\alpha - \frac{\cos\alpha}{2K}\left(\tilde{x}_0^2 + \tilde{y}_0^2\right)\right]}_{\tilde{x}_1} \right\} \exp\left(i\tilde{y}_0 y_1\right) d\tilde{y}_0 d\tilde{x}_0. \tag{10}$$

Now we make the following transformation of reciprocal coordinates

$$\begin{aligned} \tilde{x}_1 &= \tilde{x}_0 \sin\alpha - \frac{\cos\alpha}{2K}\left(\tilde{x}_0^2 + \tilde{y}_0^2\right), \\ \tilde{y}_1 &= \tilde{y}_0, \end{aligned} \tag{11}$$

with the inverse transformation

$$\begin{aligned} \tilde{x}_0 &= K\tan\alpha - \sqrt{K^2\tan^2\alpha - \tilde{y}_1^2 - \frac{2K}{\cos\alpha}\tilde{x}_1}, \\ \tilde{y}_0 &= \tilde{y}_1. \end{aligned} \tag{12}$$

The ambiguity of the sign in front of the square root that arises is resolved by choosing the minus sign, since this choice is the only consistent one with the paraxial approximation ($\tilde{x}_0 \ll K$). The jacobian of the transformation is

$$\left|\frac{\partial(\tilde{x}_0, \tilde{y}_0)}{\partial(\tilde{x}_1, \tilde{y}_1)}\right| = \frac{\partial\tilde{x}_0}{\partial\tilde{x}_1}\frac{\partial\tilde{y}_0}{\partial\tilde{y}_1} - \frac{\partial\tilde{x}_0}{\partial\tilde{y}_1}\frac{\partial\tilde{y}_0}{\partial\tilde{x}_1} = \frac{1}{\sqrt{\sin^2\alpha - \frac{\tilde{y}_1^2\cos^2\alpha}{K^2} - \frac{2\tilde{x}_1\cos\alpha}{K}}}, \tag{13}$$

and after substituting it to Eq. (10) the transformation finally results in

$$U_C(x_1, y_1) = \iint \widetilde{U}_0\left(\tilde{x}_0(\tilde{x}_1, \tilde{y}_1), \tilde{y}_0(\tilde{x}_1, \tilde{y}_1)\right) \times \frac{\exp\left\{-i\frac{z_0}{2K}\left[\tilde{x}_0^2(\tilde{x}_1, \tilde{y}_1) + \tilde{y}_1^2\right]\right\}}{\sqrt{\sin^2\alpha - \frac{\tilde{y}_1^2\cos^2\alpha}{K^2} - \frac{2\tilde{x}_1\cos\alpha}{K}}} \exp\left\{i[x_1\tilde{x}_1 + y_1\tilde{y}_1]\right\} d\tilde{y}_1 d\tilde{x}_1. \tag{14}$$

This can be rewritten in a compact form as

$$U_C(x_1, y_1) = \mathcal{F}^{-1}\left[\widetilde{U}_0\left(\tilde{x}_0(\tilde{x}_1, \tilde{y}_1), \tilde{y}_0(\tilde{x}_1, \tilde{y}_1)\right) P^{(1)}_{\alpha, z_0}\left(\tilde{x}_0(\tilde{x}_1, \tilde{y}_1), \tilde{y}_0(\tilde{x}_1, \tilde{y}_1)\right)\right]. \tag{15}$$

where we used a general quantity $P^{(1)}_{\alpha,z}$, which we refer to as a 'generalized Fresnel propagator of the first kind' defined as

$$P^{(1)}_{\alpha,z}(\tilde{x}_i, \tilde{y}_i) = \frac{\exp\left\{-i\frac{z}{2K}\left[\tilde{x}_i^2 + \tilde{y}_i^2\right]\right\}}{\sqrt{\sin^2\alpha - \frac{\tilde{y}_{i+1}^2\cos^2\alpha}{K^2} - \frac{2\tilde{x}_{i+1}\cos\alpha}{K}}}. \tag{16}$$

This propagator is used for the propagation on inclined planes, where the main propagation direction of the beam is perpendicular to the input plane. We also note that all the round brackets

Optics EXPRESS

in Eqs. (14), (15) and (16) have the meaning of functional dependence. After performing an interpolation of $\widetilde{U}_0$ values from the uniform grid points $(\tilde{x}_0, \tilde{y}_0)$ to uniform grid points $(\tilde{x}_1, \tilde{y}_1)$ based on Eq. (12), the calculation based on Eq. (15) can be performed using the Fast Fourier transform algorithm (FFT), which greatly speeds up the calculation. The inverse relationship of retrieving U_0 from U_C (backward propagation) would be analogously

$$U_0(x_0, y_0) = \mathcal{F}^{-1}\left[\frac{\widetilde{U}_C\left(\tilde{x}_1(\tilde{x}_0, \tilde{y}_0), \tilde{y}_1(\tilde{x}_0, \tilde{y}_0)\right)}{P^{(1)}_{\alpha,z_0}(\tilde{x}_1(\tilde{x}_0, \tilde{y}_0), \tilde{y}_1(\tilde{x}_0, \tilde{y}_0))}\right]. \tag{17}$$

It is to be noted that this time, the coordinate transformation based on Eq. (11) needs to used.

Now we want to further propagate the wave-field U_C to the detector plane in order to obtain U_D. The situation is equivalent to the case of retrieving U_0 from U_C, except for the opposite sign within the exponential indicating forward propagation. To this end, we similarly define a 'generalized Fresnel propagator of the second kind', which will be used for free space propagation from an inclined plane, where the main propagation direction of the beam is perpendicular to the output plane. Its formal definition is

$$P^{(2)}_{\beta,z}(\tilde{x}_i, \tilde{y}_i) = \frac{\exp\left\{+i\frac{z}{2K}\left[\tilde{x}^2_{i+1} + \tilde{y}^2_{i+1}\right]\right\}}{\sqrt{\sin^2\beta - \frac{\tilde{y}_i^2\cos^2\beta}{K^2} - \frac{2\tilde{x}_i\cos\beta}{K}}}, \tag{18}$$

and using this, the second propagation from the crystal to the detector can be written as

$$U_D(x_2, y_2) = \mathcal{F}^{-1}\left[\frac{\widetilde{U}_C\left(\tilde{x}_1(\tilde{x}_2, \tilde{y}_2), \tilde{y}_1(\tilde{x}_2, \tilde{y}_2)\right)}{P^{(2)}_{\beta,z_1}(\tilde{x}_1(\tilde{x}_2, \tilde{y}_2), \tilde{y}_1(\tilde{x}_2, \tilde{y}_2))}\right], \tag{19}$$

where the coordinate transformations are analogous to the previous case:

$$\begin{aligned} \tilde{x}_1 &= \tilde{x}_2\sin\beta - \frac{\cos\beta}{2K}\left(\tilde{x}_2^2 + \tilde{y}_2^2\right), \\ \tilde{y}_1 &= \tilde{y}_2. \end{aligned} \tag{20}$$

The key point now is that Eqs. (15) and (19) can be merged in Fourier space as

$$\begin{aligned} \widetilde{U}_D(\tilde{x}_2, \tilde{y}_2) &= \frac{\widetilde{U}_C\left(\tilde{x}_1(\tilde{x}_2, \tilde{y}_2), \tilde{y}_2\right)}{P^{(2)}_{\beta,z_1}(\tilde{x}_1(\tilde{x}_2, \tilde{y}_2), \tilde{y}_2)} = \\ &= \widetilde{U}_0\left(\tilde{x}_0(\tilde{x}_1(\tilde{x}_2, \tilde{y}_2), \tilde{y}_1), \tilde{y}_2\right)\frac{P^{(1)}_{\alpha,z_0}\left(\tilde{x}_0(\tilde{x}_1(\tilde{x}_2, \tilde{y}_2), \tilde{y}_1), \tilde{y}_2\right)}{P^{(2)}_{\beta,z_1}(\tilde{x}_1(\tilde{x}_2, \tilde{y}_2), \tilde{y}_2)}, \end{aligned} \tag{21}$$

where the coordinate functional dependancies were written here for transparency reasons only for $\tilde{x}$ coordinates, because in our special case from Fig. 1 is $\tilde{y}_0 = \tilde{y}_1 = \tilde{y}_2$ anyway. This way, one can work directly with the coordinate transformation from $(\tilde{x}_0, \tilde{y}_0)$ to $(\tilde{x}_2, \tilde{y}_2)$, with the following transformation formulas (obtained by merging Eqs. (12) and (20))

$$\begin{aligned} \tilde{x}_0 &= K\tan\alpha - \sqrt{K^2\tan^2\alpha - 2KM\tilde{x}_2\tan\alpha + \frac{\cos\beta}{\cos\alpha}\left(\tilde{x}_2^2 + \tilde{y}_2^2\right) - \tilde{y}_2^2}, \\ \tilde{y}_0 &= \tilde{y}_2. \end{aligned} \tag{22}$$

Using this we can finally write down the desired relationship as

$$U_D(x_2, y_2) = \mathcal{F}^{-1}\left[\widetilde{U}_0\left(\tilde{x}_0(\tilde{x}_2, \tilde{y}_2), \tilde{y}_2\right)\frac{P^{(1)}_{\alpha,z_0}\left(\tilde{x}_0(\tilde{x}_2, \tilde{y}_2), \tilde{y}_2\right)}{P^{(2)}_{\beta,z_1}(\tilde{x}_1(\tilde{x}_2, \tilde{y}_2), \tilde{y}_2)}\right]. \tag{23}$$

Computer implementation of Eq. (23) requires performing these steps:

Optics EXPRESS

1. Calculate FFT of $U_0(x_0, y_0)$ to yield $\widetilde{U}_0(\tilde{x}_0, \tilde{y}_0)$.
2. Create a regular grid of reciprocal coordinates $(\tilde{x}_2, \tilde{y}_2)$ and calculate their corresponding values of $(\tilde{x}_0(\tilde{x}_2, \tilde{y}_2), \tilde{y}_0(\tilde{x}_2, \tilde{y}_2))$ based on Eq. (22).
3. Perform interpolation of $\widetilde{U}_0$ values on the positions $(\tilde{x}_0(\tilde{x}_2, \tilde{y}_2), \tilde{y}_0(\tilde{x}_2, \tilde{y}_2))$ based on the known values $\widetilde{U}_0(\tilde{x}_0, \tilde{y}_0)$ (interpolation from regular grid points onto irregular grid).
4. Calculate propagators $P^{(2)}_{\beta,z_1}(\tilde{x}_1(\tilde{x}_2, \tilde{y}_2))$ and $P^{(1)}_{\alpha,z_0}(\tilde{x}_0(\tilde{x}_2, \tilde{y}_2), \tilde{y}_2)$ based on their definitions in Eqs. (16) and (18) on the sample points given by Eqs. (20) and (22), respectively.
5. Perform operations according to Eq. (23) to yield $U_D(x_2, y_2)$.

The advantage of such direct merged approach is that the computational demands are twice as low as for the case of independently applying two propagations on inclined planes according to Eqs. (15) and (19).

2.4. Adding the transfer functions of the optical elements

For the ED method, this can be easily accomplished by adding the factor $C_1(\tilde{x}_0, \tilde{y}_0)$ corresponding to the transfer function of the optical element (e.g. crystal transfer function) into the curly brackets in Eq. (8). C_1 expresses the modification of the wave-field (absorption and phase-shift) due to the crystal reflection, and can be calculated separately. Similarly, for the MFT method, we add the same factor in Eq. (3).

Adjusting the RCT method requires going back to Eq. (9), which becomes

$$U_C(x_0, y_0) = \iint \widetilde{U}_0(\tilde{x}_0, \tilde{y}_0) \exp\left[-i\frac{z_0 + z(x_0)}{2K}\left(\tilde{x}_0^2 + \tilde{y}_0^2\right)\right] C_1(\tilde{x}_0, \tilde{y}_0) \quad \times \exp\left[i(\tilde{x}_0 x_0 + \tilde{y}_0 y_0)\right] d\tilde{x}_0 d\tilde{y}_0. \tag{24}$$

After repeating the steps in Section 2.3, we finally arrive at

$$U_D(x_2, y_2) = \mathcal{F}^{-1}\left[\widetilde{U}_0\left(\tilde{x}_0(\tilde{x}_2, \tilde{y}_2), \tilde{y}_2\right) \frac{P^{(1)}_{\alpha,z_0}\left(\tilde{x}_0(\tilde{x}_2, \tilde{y}_2), \tilde{y}_2\right)}{P^{(2)}_{\beta,z_1}\left(\tilde{x}_1(\tilde{x}_2, \tilde{y}_2), \tilde{y}_2\right)} C_1(\tilde{x}_0(\tilde{x}_2, \tilde{y}_2), \tilde{y}_2)\right]. \tag{25}$$

In practice, this requires one extra interpolation of the same type as for $\widetilde{U}_0$ - interpolation using the known original values $C_1(\tilde{x}_0, \tilde{y}_0)$ (lying on a regular grid) onto the irregular grid points $C_1(\tilde{x}_0(\tilde{x}_2, \tilde{y}_2), \tilde{y}_0)$.

3. Propagation through many crystals

The RCT formalism can be further conveniently generalized for propagation through an arbitrary number of crystals. Suppose we have N crystals, each of them reflecting (and potentially also magnifying/demagnifying) the beam in either horizontal (x) or vertical (y) direction before finally reaching the detector (an example of 4 crystals is depicted in Fig. 2). An i-th crystal upstream will be characterized by its transfer function C_i, incidence angle α_i and the outcoming angle β_i, for $i = 1, \ldots, N$. Mean propagation distances of the wave-field between the sample, crystals and the detector will be denoted as $z_0, z_1, \ldots, z_N$, respectively. Analogously to the previous section, we define $2N + 1$ coordinate frames over different planes with Cartesian coordinates $(x_0, y_0); (x_1, y_1); \ldots; (x_{2N}, y_{2N})$. Their positions are as follows:

- (x_0, y_0) is the sample plane,
- (x_{2N}, y_{2N}) is the detector plane,

Optics EXPRESS

- $(x_1, y_1); (x_3, y_3); \ldots; (x_{2N-1}, y_{2N-1})$ refer to the crystal surfaces,
- $(x_2, y_2); (x_4, y_4); \ldots; (x_{2N-2}, y_{2N-2})$ refer to the planes perpendicular to the beam direction and in the middle distance between two consecutive crystals.

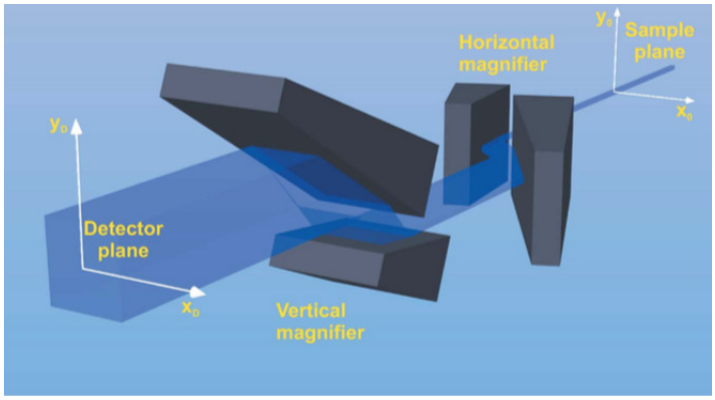

Fig. 2. Wave propagation for the situation of 4 crystals forming the Bragg magnifier. Figure taken from [9].

The relationship for forward propagation through this set of N crystals will then be

$$U_D(x_{2N}, y_{2N}) = \mathcal{F}^{-1}\left[\widetilde{U}_0\left(\tilde{x}_0^*, \tilde{y}_0^*\right) \frac{P^{(1)}_{\alpha_1,z_0}\left(\tilde{x}_0^*, \tilde{y}_0^*\right)}{P^{(2)}_{\beta_N,z_N}\left(\tilde{x}_{2N-1}^*, \tilde{y}_{2N-1}^*\right)} \times \prod_{i=1}^{N-1} \frac{P^{(1)}_{\alpha_{i+1},z_i/2}\left(\tilde{x}_{2i}^*, \tilde{y}_{2i}^*\right)}{P^{(2)}_{\beta_i,z_i/2}\left(\tilde{x}_{2i-1}^*, \tilde{y}_{2i-1}^*\right)} \prod_{i=1}^{N} C_i\left(\tilde{x}_{2i-2}^*, \tilde{y}_{2i-2}^*\right)\right], \tag{26}$$

where $\tilde{x}_j^* = \tilde{x}_j(\tilde{x}_{2N}, \tilde{y}_{2N})$ and $\tilde{y}_j^* = \tilde{y}_j(\tilde{x}_{2N}, \tilde{y}_{2N})$ for $\forall j$. In other words, all the quantities on the right side of the equation have to be calculated on the sample points that are transformed from the detector plane coordinates $(\tilde{x}_{2N}, \tilde{y}_{2N})$. In general, this can be achieved by applying the coordinate transformations in Eqs. (11) and (12) multiple times, as shown in the previous section in Eq. (22).

From the practical point of view, for a fixed setup, all the quantities $P_{\alpha,z}$ and C_i need to be calculated just once yielding an effective propagator, which can be simply reused for an arbitrary number of forward and backward wave-field propagations through the whole system. This way, the computational demands stay the same for any number of crystals in the system. Specifically, one forward or backward propagation through the whole setup only requires two 2D FFT's and one 2D interpolation (from regular grid points $\widetilde{U}_0(\tilde{x}_0, \tilde{y}_0)$ to irregular grid points $\widetilde{U}_0\left(\tilde{x}_0^*, \tilde{y}_0^*\right)$). This makes the method especially convenient for applications where one requires a fast and accurate approach for many forward and backward propagations through a complex system.

We conclude this section by shortly describing the generalization procedure for the other two methods. For the ED method, Eq. (8) can be easily modified to account for all the free space propagations present, as well as the crystal transfer functions (see e.g. in [3]). This way, similarly as for the RCT method, the computational demands are practically independent of the number of crystals. For the MFT method, one needs to repeat the procedure for one crystal multiple times, yielding inconvenient linear dependency of the computation time with the number of crystals.

Optics EXPRESS

4. Numerical tests of the methods

In order to test and compare the accuracy and speed of the described methods, several numerical tests have been performed. The phantom of interest was chosen to be a polystyrene sphere, and the parameters of the simulation were the following (chosen to closely resemble the real parameters used in the experiment described in [3]):

- The beam coming from the source is a plane wave, with a size (field of view) 0.6 mm × 0.6 mm (sampled by 1024 × 1024 pixels).
- Energy of X-ray radiation $E = 10.7$ keV.
- Sample - a polystyrene (PS) sphere with a radius $R = 60$ μm.
- The crystal configuration is as sketched in Fig. 2 - four perfect crystals made of Germanium, first two magnifying in the horizontal dimension and the other two in the vertical dimension by means of asymmetrical Bragg reflection. The given configuration is called quasi-channel-cut Bragg magnifier [9].
- Distances $z_0 = 20$ cm and $z_1 = z_2 = z_3 = z_4 = 10$ cm.
- We used 220 crystal Bragg reflection with incident angles (with respect to crystal surface) $\alpha_1 = \alpha_3 = 0.4°, \alpha_2 = \alpha_4 = 9.7°$ and outcoming angles $\beta_1 = \beta_3 = 33.1°, \beta_2 = \beta_4 = 23.8°$.
- Crystal transfer functions C_i were calculated using the two-beam Dynamical theory of diffraction [13], and the crystals were aligned to maximize the reflected intensity.

Figure 3 shows the amplitude and the phase of our phantom on the sample plane. It is further propagated to the detector through the setup in Fig. 2 using the three methods described in Section 2. The calculated intensity patterns are shown in Fig. 4. For the RCT method, we used a cubic interpolation, since it provided the best ratio for computational demands and accuracy. No differences are observed at first sight in Fig. 4, but after plotting the absolute values of the differences (Fig. 5), the nontrivial deviations were observed with the ED method, because of the varying propagation distances. On the other hand, the results with the RCT method exhibit practically no deviation from the results with the reference method MFT. To emphasize this effect, the line profile (along the yellow lines in Fig. 4) is shown in Fig. 6. For the ED method, the positions of Fresnel fringes are shifted more and more as one moves from the image center. On the contrary, the RCT method provides a perfect fit for the data obtained with the MFT method. It is to be noted, that using different standard test patterns (e.g., a square) produced quantitatively similar results as presented in Fig. 5.

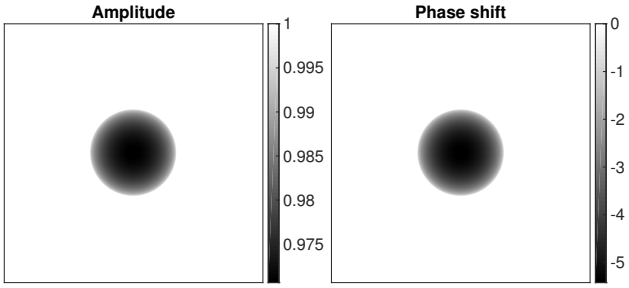

Fig. 3. The amplitude and the phase of the polystyrene sphere - our phantom object, i.e. the wave-field $U_0(x_0, y_0)$.

Optics EXPRESS

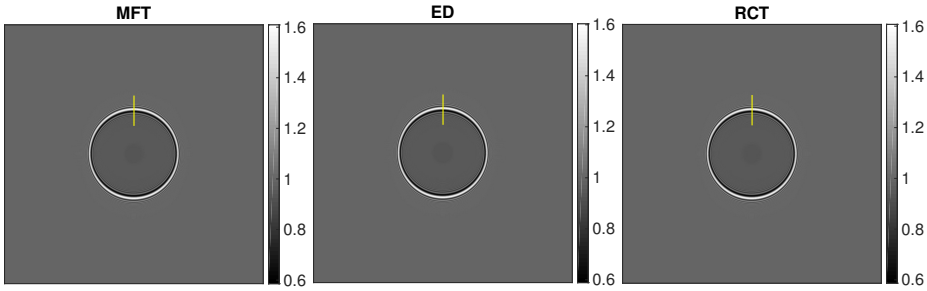

Fig. 4. Simulated intensity patterns $|U_D(x_2, y_2)|^2$ for all three described methods. The yellow lines show the position of the profile lines plotted in Fig. 6.

We also measured the time required for one forward propagation. All three methods were tested on the same PC with standard contemporary specifications (CPU - Intel Core i7, 2 GHz), and the implementation of the methods was done with Matlab. The time for the ED method was (0.04 ± 0.01) s, for the RCT method (0.13 ± 0.02) s, and for the MFT method around 300 s. This underlines the usefulness of our RCT method, which is 1-2 orders of magnitude more

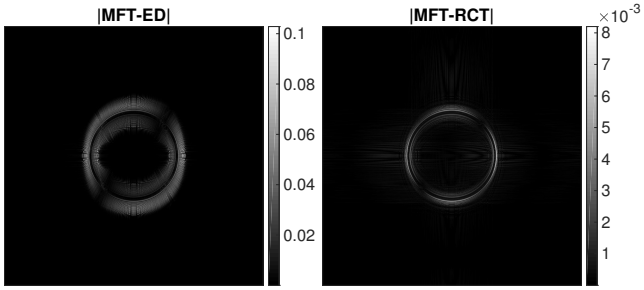

Fig. 5. The absolute value of the difference in detector intensities between the results obtained with the ED and RCT methods, in comparison to the reference method MFT. The superiority of the RCT method is clearly visible.

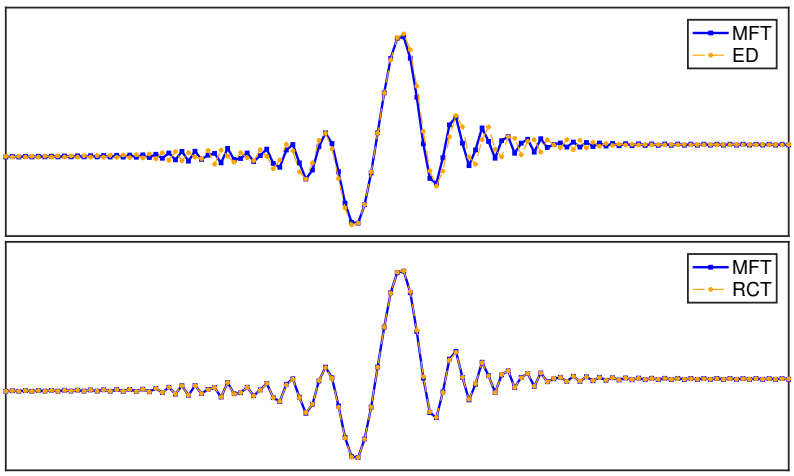

Fig. 6. The line profiles along the yellow lines in Fig. 4.

Optics EXPRESS

accurate than the ED method while being just about three times slower.

5. Conclusion

We closely studied the wave propagation through one or more consecutive reflecting planes, e.g. crystals in Bragg geometry subjected to X-ray radiation. Three methods of coping with this problem were described and mutually compared in terms of accuracy and speed. The first two methods, the Effective Distance (ED) method, and the Many Fourier Transforms (MFT) method, have been also used before, while the third method, named the Reciprocal Coordinate Transform (RCT) method, has been developed and is the main novelty of this paper. RCT method uses coordinate transformation to rewrite the diffraction integral in the form of the Fourier Transform, exploiting its computational speed. Conveniently, it can be generalized for wave propagation through an arbitrary number of consecutive crystals while having the computational demands independent of the number of crystals.

Numerical tests have revealed the superiority of the RCT method by 1-2 orders of magnitude in terms of accuracy when compared to the ED method, and in terms of speed when compared to the MFT method. Being just three times slower than the ED method (which uses limiting approximation), RCT method provides an excellent method for fast and accurate forward and backward wave propagations through a set of crystals. One of the direct applications of the method is in X-ray imaging using the Bragg magnifier, specifically in simulations of image formation as well as in phase retrieval.

Funding

EU FP7-REGPOT "Fostering Excellence in Multiscale Cell Imaging" (CELIM); VVGS-PF-2015-470.

References

1. S. Marchesini, H. He, H. N. Chapman, S. P. Hau-Riege, A. Noy, M. R. Howells, U. Weierstall, and J. C. H. Spence, "X-ray image reconstruction from a diffraction pattern alone," Phys. Rev. B **68**, 140101 (2003).
2. D. Paganin, *Coherent X-Ray Optics* (Oxford University, 2006).
3. S. Hrivňak, J. Uličný, L. Mikeš, A. Cecilia, E. Hamann, T. Baumbach, L. Švéda, Z. Zápražný, D. Korytár, E. Gimenez-Navarro, U. H. Wagner, C. Rau, H. Greven, and P. Vagovič, "Single-distance phase retrieval algorithm for Bragg magnifier microscope," Opt. Express **24**, 27753–27762 (2016).
4. P. Vagovič, L. Švéda, A. Cecilia, E. Hamann, D. Pelliccia, E. N. Gimenez, D. Korytár, K. M. Pavlov, Z. Zápražný, M. Zuber, T. Koenig, M. Olbinado, W. Yashiro, A. Momose, M. Fiederle, and T. Baumbach, "X-ray Bragg magnifier microscope as a linear shift invariant imaging system: image formation and phase retrieval," Opt. Express **22**, 21508–21520 (2014).
5. P. Modregger, D. Lübbert, P. Schäfer, and R. Köhler, "Magnified x-ray phase imaging using asymmetric Bragg reflection: Experiment and theory," Phys. Rev. B **74**, 054107 (2006).
6. N. Delen and B. Hooker, "Free-space beam propagation between arbitrarily oriented planes based on full diffraction theory: a fast fourier transform approach," J. Opt. Soc. Am. A **15**, 857–867 (1998).
7. N. Delen and B. Hooker, "Verification and comparison of a fast fourier transform-based full diffraction method for tilted and offset planes," Appl. Opt. **40**, 3525–3531 (2001).
8. P. Modregger, D. Lübbert, P. Schäfer, R. Köhler, T. Weitkamp, M. Hanke, and T. Baumbach, "Fresnel diffraction in the case of an inclined image plane," Opt. Express **16**, 5141–5149 (2008).
9. P. Vagovič, D. Korytár, A. Cecilia, E. Hamann, L. Švéda, D. Pelliccia, J. Härtwig, Z. Zápražný, P. Oberta, I. Dolbnya, K. Shawney, U. Fleschig, M. Fiederle, and T. Baumbach, "High-resolution high-efficiency X-ray imaging system based on the in-line Bragg magnifier and the Medipix detector," J. Synchrotron Radiat. **20**, 153–159 (2013).
10. S. Hrivňak, A. Hovan, J. Uličný, and P. Vagovič, "Phase retrieval for arbitrary Fresnel-like linear shift-invariant imaging systems suitable for tomography," Biomed. Opt. Express **9**, 4390–4400 (2018).
11. A. Authier, *Dynamical Theory of X-ray Diffraction* (Oxford University, 2004).
12. R. D. Spal, "Submicrometer resolution hard x-ray holography with the asymmetric Bragg diffraction microscope," Phys. Rev. Lett. **86**, 3044–3047 (2001).
13. X. Huang and M. Dudley, "A universal computation method for two-beam dynamical X-ray diffraction," Acta Crystallogr. Sect. A **59**, 163–167 (2003).